Lat. Am. J. Aquat. Res., 42(4): 857-870, 2014
"Oceanography and Marine Resources of Oceanic Islands of Southeastern Pacific"
M. Fernández & S. Hormazábal (Guest Editors)
DOI: 10.3856/vol42-issue4-fulltext-12

Research Article

Origin of the Easter Submarine Alignment: morphology and structural lineaments

Cristián Rodrigo[1], Juan Díaz[2] & Antonio González-Fernández[3]
[1]Facultad de Ingeniería-Geología, Universidad Andrés Bello, Quillota 980, Viña del Mar, Chile
[2]Escuela de Ciencias del Mar, Pontificia Universidad Católica de Valparaíso
Av. Altamirano 1480, Valparaíso, Chile
[3]División Ciencias de la Tierra, Centro de Investigación Científica y Educación Superior de Ensenada
Carretera Ensenada-Tijuana 3918, Ensenada, B.C., México

ABSTRACT. The Easter submarine alignment corresponds to a sequence of seamounts and oceanic islands which runs from the Ahu-Umu volcanic fields in the west to its intersection with the Nazca Ridge in the east, with a total length of about 2.900 km and a strike of N85°E. Recent bathymetric compilations that include combined satellite derived and shipboard data (Global Topography) and multibeam bathymetric data (from NGDC-NOAA) are interpreted both qualitatively and quantitatively by using a morphological analysis, which was comprised of the determination of bathymetric patterns, trends in lineations and structures; height measurements, computation of basal areas and volumes of seamounts, in order to establish clues on the origin of this seamount chain and to establish relationships with the regional tectonics. In the study region 514 seamounts were counted, of which 334 had a basal area less than the reference seamount (Moai). In general, the largest seamounts (>1000 m in height) tend to align and to have a larger volume, with an elongation of their bases along the seamount chain. On the other hand, smaller seamounts tend to be distributed more randomly with more circular bases. As a consequence of the morphological analysis, the best possible mechanism that explains the origin of the seamount chain is the existence of a localized hotspot to the west of the Salas y Gómez Island. The corresponding plume would contribute additional magmatic material towards the East Pacific Rise through canalizations, whose secondary branches would feed intermediate volcanoes. It is possible that within the Easter Island region there would be another minor contribution through fractures in the crust, due to the crustal weakening that was produced by the Easter Fracture Zone.

Keywords: seamounts, hotspot, bathymetry, morphology, Easter Island, Salas y Gómez Island.

Origen del Alineamiento Submarino de Pascua: morfología y lineamientos estructurales

RESUMEN. El alineamiento submarino de Pascua es un cordón de montes submarinos e islas que comprende, por el W, desde los campos volcánicos Ahu-Umu y, hasta el E, su intersección con la elevación de Nazca, con una extensión total de *ca*. 2900 km y un rumbo de ~N85°E. Compilaciones recientes de batimetría que incluyen datos derivados de satélites y obtenidos por buques (Global Topography) y datos batimétricos de ecosondas multihaz (NGDC-NOAA), se interpretaron cualitativa y cuantitativamente mediante análisis morfológico que consistió en la determinación de patrones batimétricos; tendencias de los lineamientos y estructuras; mediciones de alturas, áreas basales y cálculo de volúmenes de montes submarinos; para establecer indicios sobre el origen del alineamiento y asociaciones con la tectónica regional. Se contabilizaron 514 montes submarinos en la región de estudio, de los cuales 334 tuvieron un área basal menor que el monte de referencia (Moai). En general, los montes más grandes (>1000 m de altura) tienden a alinearse y a tener un mayor volumen, con un alargamiento de sus bases en el sentido de la tendencia, en cambio los menores, tienden a distribuirse más aleatoriamente, siendo sus bases más redondeadas. Como consecuencia del análisis morfológico, el mejor mecanismo que explicaría el origen de las cadenas volcánicas, sería por la existencia de un punto caliente localizado al W de la isla Salas y Gómez. Esta pluma también aportaría material magmático adicional hacia la dorsal del Pacífico oriental a través de canalizaciones, cuyas ramas secundarias alimentarían volcanes intermedios. Es posible que en el área de la Isla de Pascua exista otro aporte menor por fracturas de la corteza dado el debilitamiento cortical que produjo la Zona de Fractura de Pascua.

Palabras clave: montes submarinos, punto caliente, batimetría, morfología, Isla de Pascua, Isla Salas y Gómez.

Corresponding author: Cristian Rodrigo (cristian.rodrigo@unab.cl)

INTRODUCTION

The Easter Island and Salas y Gómez Island form a part of the chain of seamounts or volcanoes (González-Ferrán, 1987, 1994), known as "Easter-Salas y Gómez Seamount Chain" (*e.g.*, Kingsley & Schilling, 1998; Simons *et al*., 2002), "Easter Seamount Chain" (Naar *et al*., 1993; Rappaport *et al*., 1997), "Easter Ridge" o "Salas y Gómez Ridge" (Clark & Dymond, 1977), or "Easter Island Fracture Zone" (Menard, 1964), among other names.

This chain extends over 2900 km from Easter Island up to its joining point with the Nazca Ridge (Fig. 1) and is formed by large seamounts, which can reach heights of more than 3000 m above the adjacent seafloor. This chain crosses the East Pacific Rise at about 27°S (González-Ferrán, 1994). The average width of this seamount chain is about 200 km. The trend along a W-E line over the Nazca Plate has caused this topographic feature to be called "Alineamiento Submarino de Pascua" (Easter Submarine Alignment; Morales, 1984; Morales & Rodrigo, 1993-1994). This name will be used in the present work.

Rodrigo (1994) determined that the distribution of the different types of seamounts, according to their morphology and height, is irregular, in spite of their general linear distribution, showing the complex origin of this alignment. According to their dimensions, this is classified as a first order structure when considering the Southern Pacific Ocean basin and as a second order structure when considering all the world ocean basins (Lugo, 1986). It has been speculated that this alignment could extend farther to the east of the San Félix Island and San Ambrosio Island, and could even continue beneath the South American continent, and also more to the west, beyond the Pitcairn Islands (Bonatti *et al.*, 1977).

The geologic and geodynamic processes of the lithosphere can leave traces on the seafloor. For example, the analysis of the distribution and shapes of the structures generated by these processes can give clues on the tectonic evolution and the processes of formation of topographic features. The region of Easter Island and Salas y Gómez Island is characterized by the proximity of: 1) East Pacific Rise, 2) Easter Microplate, 3) Easter Fracture Zone, and 4) seamount chain. Moreover, tectonic processes have occurred and continue to occur in the area, such as plate reorganizations, jumps in ridge activity and propagating rifts segments, which result in a complex submarine geomorphology (Rodrigo, 2000). Therefore, in this work we utilize public databases and bathymetric background information to derive topographic patterns, which in turn permit us to establish clues on the origin of the Easter Submarine Alignment and relationships with the regional tectonics, focusing approximately in the region of the Chilean Economic Exclusive Zone.

Regional tectonic setting

In study region, the Nazca, Easter and Pacific plates converge against each other. The Easter Island and Salas y Gómez Islands are located on the Nazca Plate (Fig. 1). The SE border of the Easter Microplate (eastern rift) is in the NW sector of this region (Hey *et al*., 1985: Naar & Hey, 1991); to the SW and as continuation of the eastern rift, are segments of the East Pacific Rise (EPR), which are connected to the eastern rift of the Juan Fernandez Microplate (Fig. 4) (Searle 1989; Searle *et al*., 1993). In this sector the oceanic crust spreads at rate of 149 km Myr^{-1} (Martínez *et al*., 1997). The average spreading rate between the Pacific and Nazca plates is close to 150 km Myr^{-1} (Naar & Hey, 1986; Hey *et al*, 1995); and at latitude 28.5°S it is of 180 km Myr^{-1} according to Schilling *et al*. (1985). Therefore this region has the highest rate of crust formation in the Pacific Basin (Rappaport *et al*., 1997; Hey *et al.*, 2004).

In this region, the complex dynamic effects modified the morphology of a typical mid-ocean ridge 2 Myr ago and generated overlapped ridge segments of various sizes which produce a tendency to rotate the oceanic crust, which finally influenced to the formation of the Easter Microplate and the disappearance of the transform fault that joined the original ridge segments (Naar & Hey, 1991; Hey *et al.*, 1995). The microplates play an important role in the reorganizations of the largest plates. The microplates along the mid-ocean ridges have existed for several millions years while the spreading center relocates in a new position because of a large-scale jump of the ridge axis (Naar, 1992). Therefore, the borders of the Easter Microplate are composed of several segments of propagating rifts, transform faults, fracture zones and other structures (Hey *et al.*, 1985). The interaction of the propagating rifts, *i.e.*, the ridges in which part of their magmatic flux is propagating towards the axis of the ridge axis, forms "V"-shape structures (pseudofaults) over the ocean floor (Hey, 1977). The existence of these pseudofaults has been demonstrated by magnetic studies in the region of the Easter Microplate (Naar & Hey, 1986). The pseudofaults show the lithosphere envelope formed by the axis of the propagating rift and how the spreading rate decreases. These pseudofaults are similar to the fossil traces of the overlapped spreading centers (OSC), except that the former leave a morphologic and magnetic pattern, where the tip of the propagating axis is steered towards the oldest lithosphere, forming the already mentioned "V" shape (Hey, 1977; Naar, 1992).

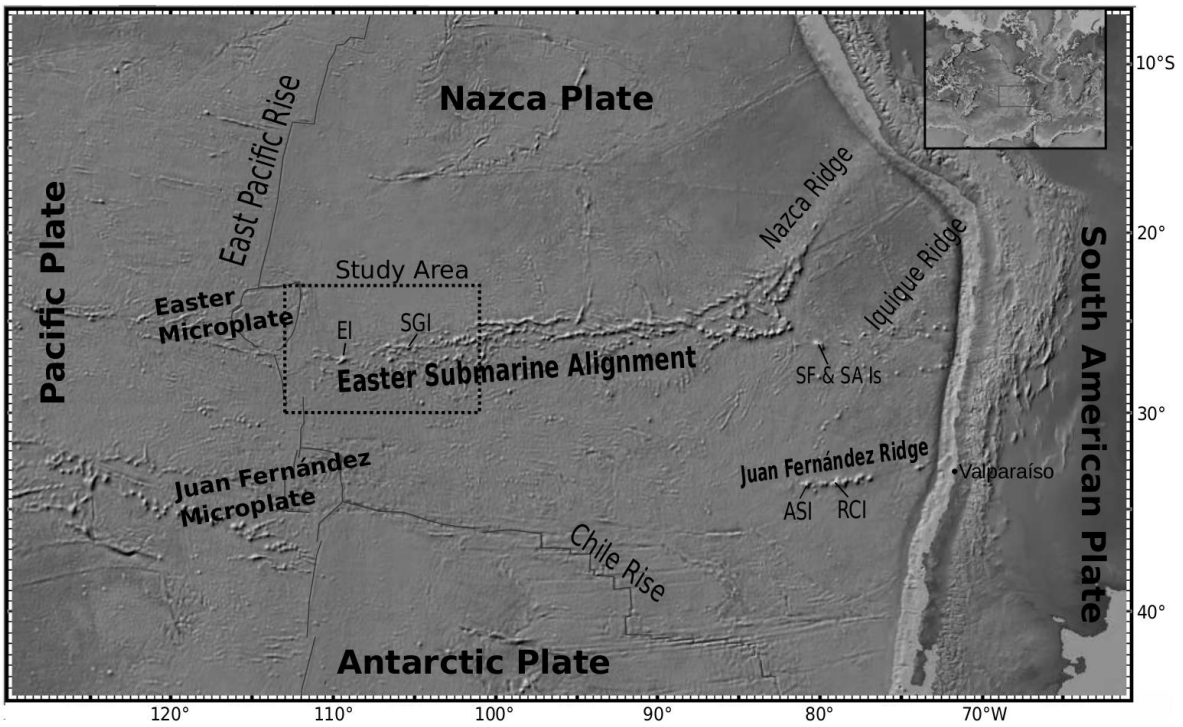

Figure 1. Map of the topography of the southeastern Pacific created using the Global Topography 15.1 database. Plates and microplates, mid-ocean ridges, aseismic ridges and seamount chains are indicated. The study area is indicated by the dotted. There are also shown San Félix Island (SF), San Ambrosio Island (SA), Alejandro Selkirk Island (ASI), Robinson Crusoe Island (RCI), Easter Island (EI) and Salas y Gómez Island (S y GI).

Macdonald (1989) explains that the formation of the observed segment for the EPR follows the emplacement of magmatic chambers spaced and shallow, with a discrete distribution along the axis. In the case of the region close to the study area, this is located to the south (between 28.5° and 30°S) and the EPR is separated into large segments (Hey *et al*., 2004). These segments propagate in the same way as the segments of the Easter Microplate and form an OSC separated by 120 km. This system is characterized by being tectonically unstable and by its continuous spreading that causes the topographic high associated with the segment that is displaced from the magma supplying area, remaining abandoned from this type of activity (fossil). After, new topographic highs are built (segments) in the location of the magmatic activity (Macdonald, 1989; Martínez *et al*., 1997).

Origin of the Easter Submarine Alignment

The explanation for the formation of the islands and the seamount chain that extends towards Chile along the Nazca Plate is still under debate. Several mechanisms have been suggested for the formation of the Easter alignment.

Morgan (1972) proposed that the Easter Seamount Chain was formed by a fixed hotspot relative to the mantle. Pilger & Handschumacher (1981) tried to develop a simple hotspot model for the Nazca Ridge and the Easter Seamount Chain, localizing the hotspot over the western rift of the Easter Microplate. However, serious kinematic problems occurred when their model was adjusted to a unified model. Therefore, Pilger & Handschumacher (1981) built an alternative model, resulting in a better fit for the Nazca Ridge, localizing the hotspot directly to the east of Salas y Gómez Island. Okal & Cazenave (1985) also located the hotspot of the Salas y Gómez Island based on magnetic anomalies data.

Modern geochemical data obtained at the East Pacific Rise, Easter Island, Salas y Gómez Island and at other points of the chain also indicate that the hotspot could be located close to Salas y Gómez Island, potentially with a channelized flux towards the Easter Microplate Rift (Kingsley & Schilling, 1998; Kingsley *et al.*, 2002; Hall & Kincaid, 2004). Recently, Ray (2012) confirmed that the hotspot could be in the sector of Salas y Gómez Island by using a geochemical and geochronological study of lavas obtained at various

points along the chain, including the Nazca Ridge. The latter does not coincide with what has been argued by some investigators, who claim that the hotspot would be beneath Easter Island or the Ahu Volcanic Field (200 km westwards from Easter Island) (*e.g.*, Hagen *et al*., 1990; Haase & Devey, 1996) or others who claim that it should be beneath the Southern East Pacific Rise (*e.g.*, Clouard & Boneville, 2001).

Given that volcanism found along the Easter Seamount Chain is anomalously young, another formation mechanism is assumed to exist. One hypothesis is the "hotline" from Bonatti *et al*. (1977), who adopted the theory of Richter (1973) of double convection of the mantle, and suggested that the chain was been created by the upwelling of part of the magmas brought by these convective cells transverse to the plate movement. Another old hypothesis, which was also previously explained, is the "leaking fracture zone" or canalizations (Menard & Atwater, 1968; Herron, 1972; Clark & Dymond, 1977).

Due to advances in the processing and resolution of satellite altimetry and the discovery of the linearity of gravimetric anomalies, other hypothesis have been postulated, such as the "linear zones of lithospheric spreading" (Mammerickx & Sandwell, 1986; Sandwell *et al.*, 1995), which could result in the incipient plate separation; however, given the lack of seismic records, the existence of normal faults have not been proven, which could, in turn, give some evidence for this hypothesis.

MATERIALS AND METHODS

Bathymetric data

Before utilizing any bathymetry database, we compared among them in order to find the best one for both resolution and data quality. For this purpose public data from several sources were used. The first database consisted of original bathymetry measured with single-beam or multibeam echosounders. These data were obtained from the U.S. National Geophysical Data Center (NGDC) website, which is part of the National Oceanic and Atmospheric Administration (NOAA). A filter was applied to these data in order to remove every unreal value (outside the range 0 m to 7000 m). Also, the multibeam data were averaged every 5 pings and data was not considered if the vessel speed was less than 2 knots. With these data, a bathymetric grid was built with a cell size of 15"x15" of arc. This grid was built using the software GMT and the interpolation algorithm called "continuous curvature splines in tension" (Smith & Wessel, 1990). Figure 2 shows the bathymetric coverage of these data.

The second type of database considered corresponded to global grids generated already by various institutions. The objective of this stage was to use data that could complement or fill the gaps in the bathymetric grid obtained from shipboard data, and also to have a lower resolution grid and of smaller digital size for a more efficient manipulation and for the creation of bathymetric maps with smoother contours. These grids were obtained from NOAA-NGDC and from the Satellite Geodesy group of the Scripps Institution of Oceanography of the University of California San Diego. For the comparison, the following grids were considered: ETOPO1 (Amante & Eakins, 2009), Global Topography v15.1-2012 (Smith & Sandwell, 1997), SRTM30 Plus v8-2012 (Becker *et al*., 2009). After the comparison, it was observed that all these grids have almost the same data for the seafloor, which include: singlebeam and multibeam bathymetry and bathymetry derived from satellite altimetry measurements. However, the SRTM30 Plus grid had the best resolution (30"x30" of arc or about 0.9x0.9 km) and thus it was the one utilized for the analysis. Finally the grid computed from shipboard data (single beam and multibeam) was superimposed on top of the SRTM30 Plus grid.

Analysis of bathymetric data

The analysis of the data was based on the identification of topographic lineations, structures and seamounts, and measurements of basal area and heights were made, complementing and updating the work carried out by Rodrigo (1994, 2000) and Rappaport *et al*. (1997). The seamount database Seamount Biogeosciences Network (http://earthref.org/SC/) was also used.

The methodology employed for the determination of the dimensions and shapes of the seamounts was based on Rappaport *et al*. (1997). These authors considered seamounts with heights greater than 200 m. The reason for this criterion is that they acquired bathymetry from the GLORI-B side-scan sonar, which had good lateral coverage, but with less spatial resolution than multibeam bathymetry. Therefore only seamounts with heights greater than 200 m were considered. In our case, where we have used satellite-derived bathymetry, the resolution is lower than for the multibeam bathymetry. Using visual comparison, seamounts with heights greater than 500 m were well determined. However, for the morphologic analysis, only seamounts with height greater than 1000 m were considered, using the Moai seamount as a reference, because of its representative size and shape. That is, seamounts with basal areas larger than that of Moai were classified as "large seamounts" and seamounts with basal areas less than that of Moai were classified

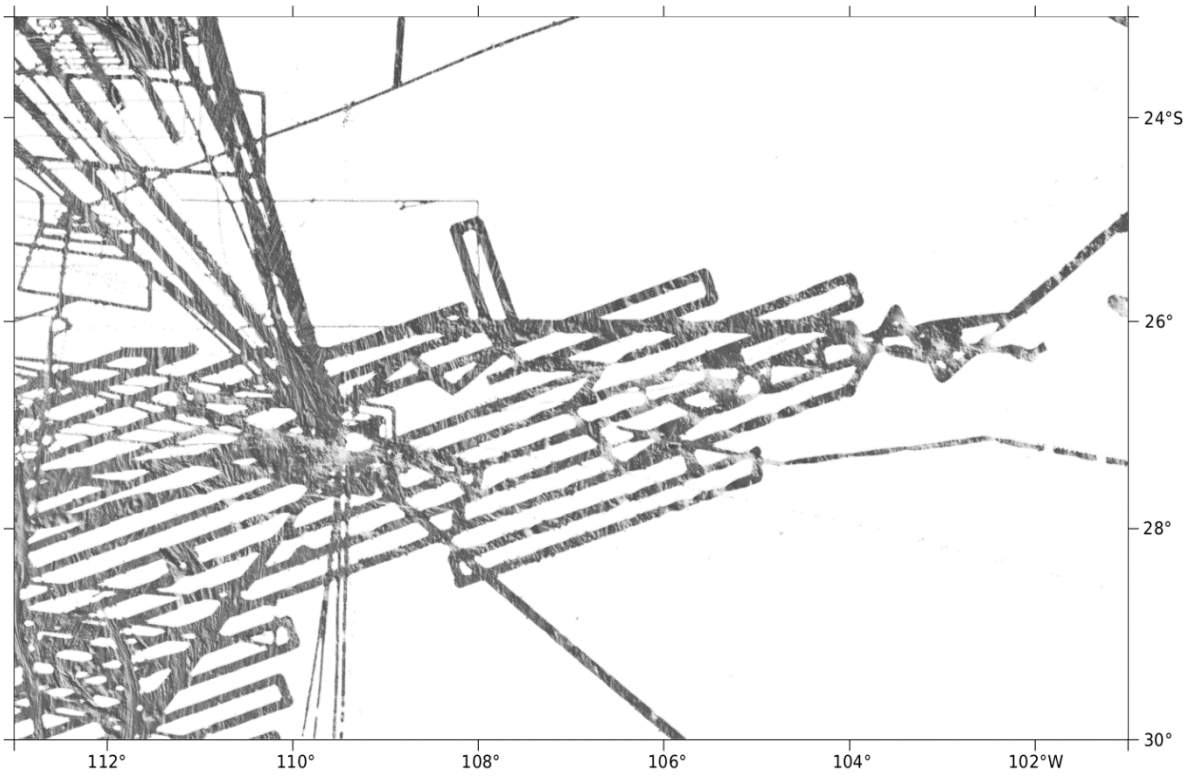

Figure 2. Bathymetric map of the original single beam and multibeam bathymetry data downloaded from the NGDC-NOAA website. These data fail to completely cover the study area.

as "small seamounts". A description of small seamounts can be found in Rappaport *et al*. (1997).

In general, the identification of seamounts and structures and their measurements were carried out by inspection of the topographic maps and a 3D model, visualized with the software iView4D (www.qps.nl). The determination of the base of the seamounts was accomplished by finding the change in slope at the foot of seamounts, considering an average level for the adjacent depths, given the roughness of the seafloor and of the seamounts. To compute volume it was assumed that the seamounts were perfectly conic.

RESULTS

Bathymetry and topographic alignments of the region

In general, the study region can be divided into three bathymetric trends: a central sector in a E-W direction with large variability in the bathymetry caused by the presence of a chain of islands and seamounts; a northern sector, which has a gentle slope from S to N, starting at the northern flank of the chain at 3500 m depth; and a western sector, where the East Pacific Rise and the eastern rifts of the Easter Microplate dominate, and where the ridge segments have typical depths of less than 2500 m (Fig. 3). In the study area depths between 2950 and 3700 m prevail (Fig. 4). Taking into account the height of the islands, the mean depth of the region is 3239 m, with a standard deviation of 458 m.

The Easter Submarine Alignment has a general strike of N85°E (Fig. 5), but two different strikes can be identified if the alignments of the largest seamounts are considered: (1) from the volcanic fields of Ahu and Umu (Hagen *et al*., 1990) up to longitude 107.5°W, with a strike of N105°E; and (2), from longitude 107°W towards the E, with a strike of N85°E (Fig. 5), which has a similar strike to the Juan Fernández Ridge (Rodrigo & Lara, 2014). There are other topographic alignments with important structures, but these have a strike rather NW-SE and others almost N-S (Fig. 5).

The linear trend of the volcanic fields of Ahu and Umu with Easter Island have a similar strike to that of the Easter Fracture Zone (Easter FZ, Fig. 5) or SOEST (Hey *et al*., 1995), including other parallel topographic alignments. From Figure 5 it is also possible to identify V-shaped pseudofaults (*e.g.*, Naar & Hey, 1986; Hey *et al*., 1995), which have their bases at 27°S, and ridge segments, including the spreading overlapping centers

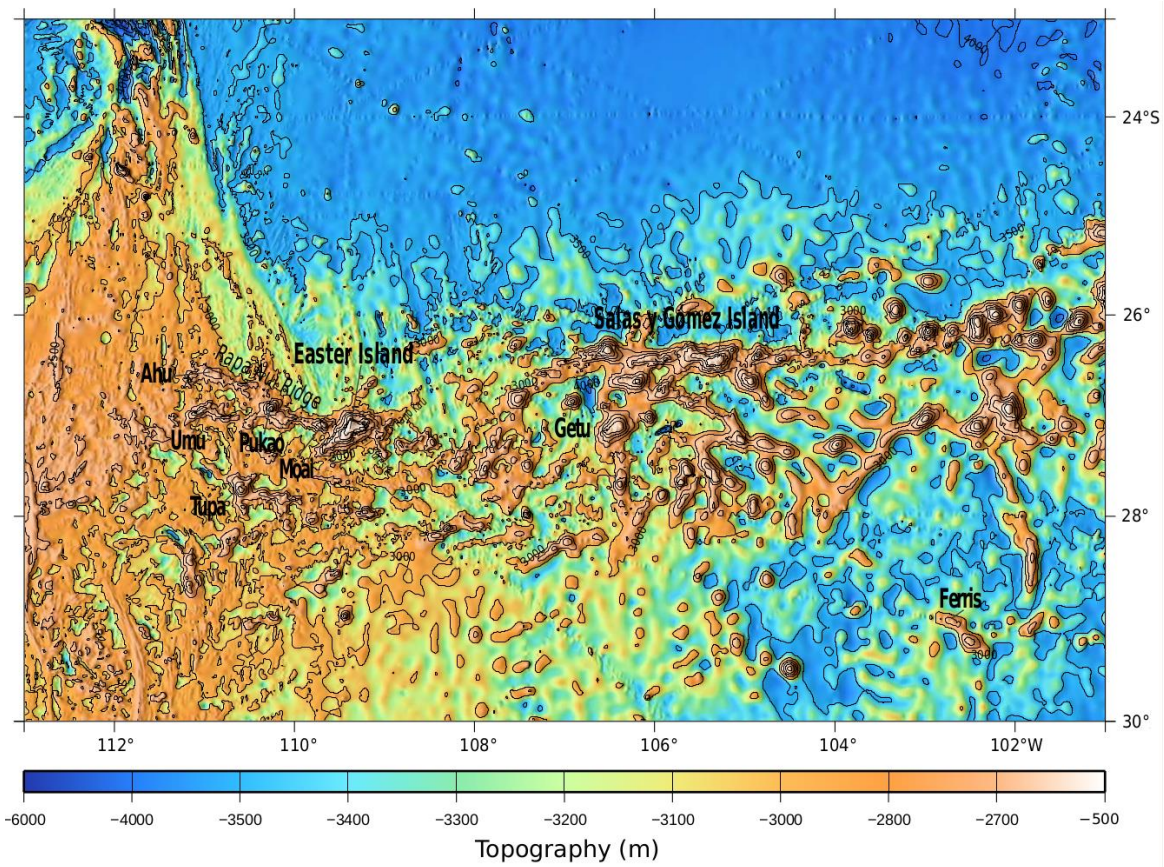

Figure 3. Bathymetric map of the study area resulting from the compilation of data derived from satellite data and single beam and multibeam echo sounder measurements. Bathymetric contours every 500 m.

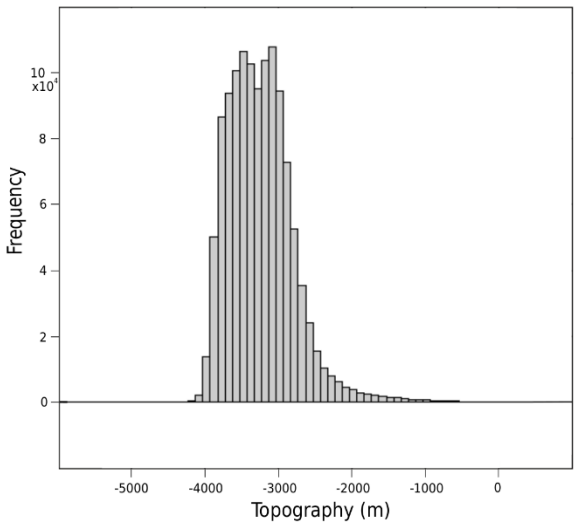

Figure 4. Histogram of absolute frequency of the bathymetry of the study area. The distribution is mostly concentrated at depths between 2950 m and 3700 m.

of the seafloor (OSC) (*e.g.*, Naar & Hey, 1986; Martínez *et al.*, 1997; Baker *et al.*, 2002; Hey *et al.*, 2004). Other minor linear trends can be identified through the use of multibeam bathymetry. These topographic alignments are approximately parallel to the ridge segments and to the pseudofaults, showing that their origin took place at the axis of the mid-ocean ridge (Fig. 5).

The bases of the seamounts are joined at depths between approximately 2900 and 3000 m (Figs. 3, 5). These bases are elongated and narrow, but continuous, with an average diameter of about 37 km. At depths less than 2800 m the continuity between Easter Island and the longitude ~108°W disappears, but to the East (towards Salas y Gómez Island) it remains.

Seamounts of the Easter Island group

The highest point of the study area is defined by Easter Island, which reaches over 400 m above sea level. To the west of the island there is the Moai Seamount, which reaches a height over 2000 m above the 3000 m sea floor depth level, as was described before (Fig. 3). A prolongation of its base is observed towards the NW until it reaches another seamount of similar charac-teristics, but with a larger base. This is the Pukao Seamount (Hagen *et*

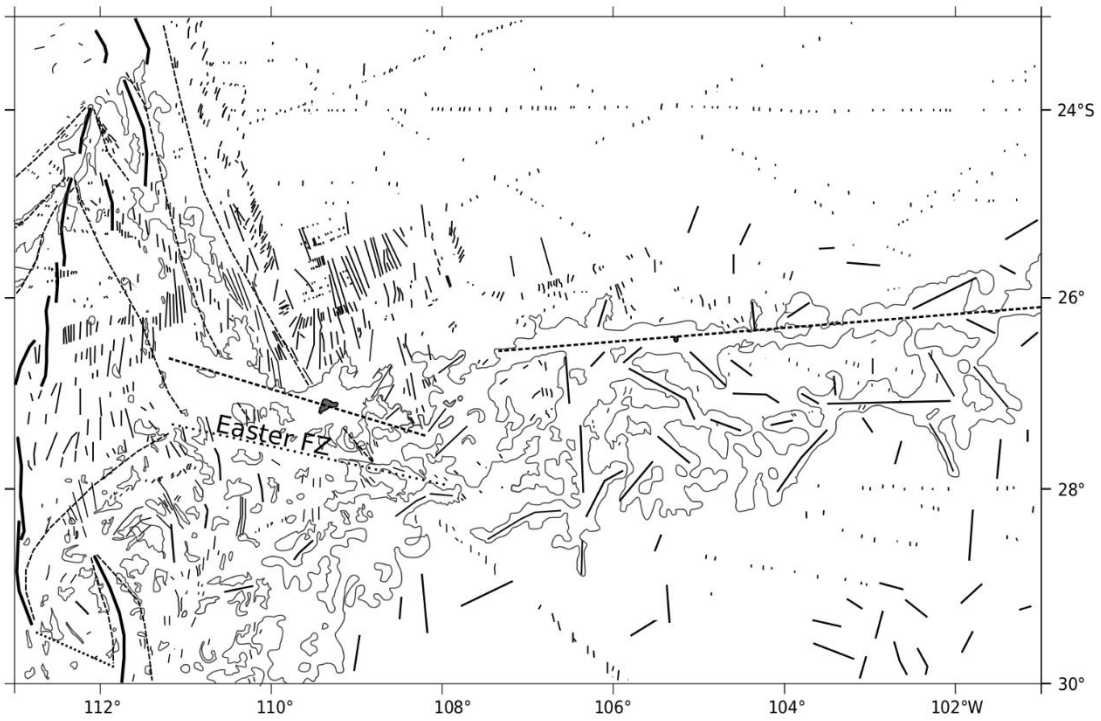

Figure 5. Map of lineaments of the study area (updated from Rodrigo, 2000). Ridge segments are thick solid lines; high elevations are solid lines of intermediate thickness; lower elevations or roughness of the seafloor are thin solid lines; depressions are dotted lines; pseudofaults are long dashed lines; and chain trends are segmented lines short and wide. Continuous base of the chains is also shown considering the 2900-3000 m isobath depth.

al., 1990). With a similar tendency in the strike of the former elevations, there is the Ahu-Umu Volcanic Field (Figs. 3, 5). This extends over almost 130 km towards the west from Easter Island and covers approximately 2500 km^2. It is built up of numerous and small volcanic cones (Hagen *et al*., 1990), which are not possible to distinguished with the available data. This group of seamounts has been called the Rapa Nui Alignment (Fig. 3).

Easter Island also shows two prolongations towards the SE and SW, which form a chain of elevations with heights less than that of the Moai Seamount. These elevations, such as the southeast and Rano Kau, have been identified by Hagen *et al*. (1990). More to the south of Easter Island there are other seamounts with similar characteristics to the Moai and Pukao seamounts. The largest one is located at approximately 27.78°S and 110.6°W. It has a basal diameter of almost 30 km with an E-W direction. In its SE part there is a prolongation of its base, forming a smaller elongated elevation, with a similar morphology and orientation as the ones described for the Moai and Pukao seamounts and for the Ahu Volcanic Field. To the south of the Umu Volcanic Field it is possible to identify the Easter Fracture Zone that runs from the point 27.9°S, 108°W until the point 27.3°S, 111.6°W (Figs. 3, 5).

Morphology and distribution of the seamounts in the region

Considering area B in Figure 6, 514 seamounts were counted (including the islands). Area A is the one analyzed by Rappaport *et al*. (1997). Using the Moai Seamount as a reference, there are 36 seamounts with a larger basal area, and 334 seamounts with a smaller basal area; so that for the study region the seamounts with smaller basal area dominate. From Figure 6 one can see that the large seamounts are those that form principal alignments and the smaller seamounts are more dispersed or have linear tendencies with different orientations.

Taking into account only the seamounts that form the largest E-W alignments (seamounts numbered in Fig. 6), one can distinguish that the bases tend to be more circular, but at the same time they tend to be more elongated in an E-W direction. In effect, between the longitudes 108° and 103°W, in the sector of Salas y Gómez Island, the largest seamounts have a tendency for an E-W elongation (Fig. 5), but towards the E, they tend to elongate individually with a N-S strike. The topographic NW-SE trends identified in the former section that come out of the main alignment are also relevant for seamount elongation along this direction.

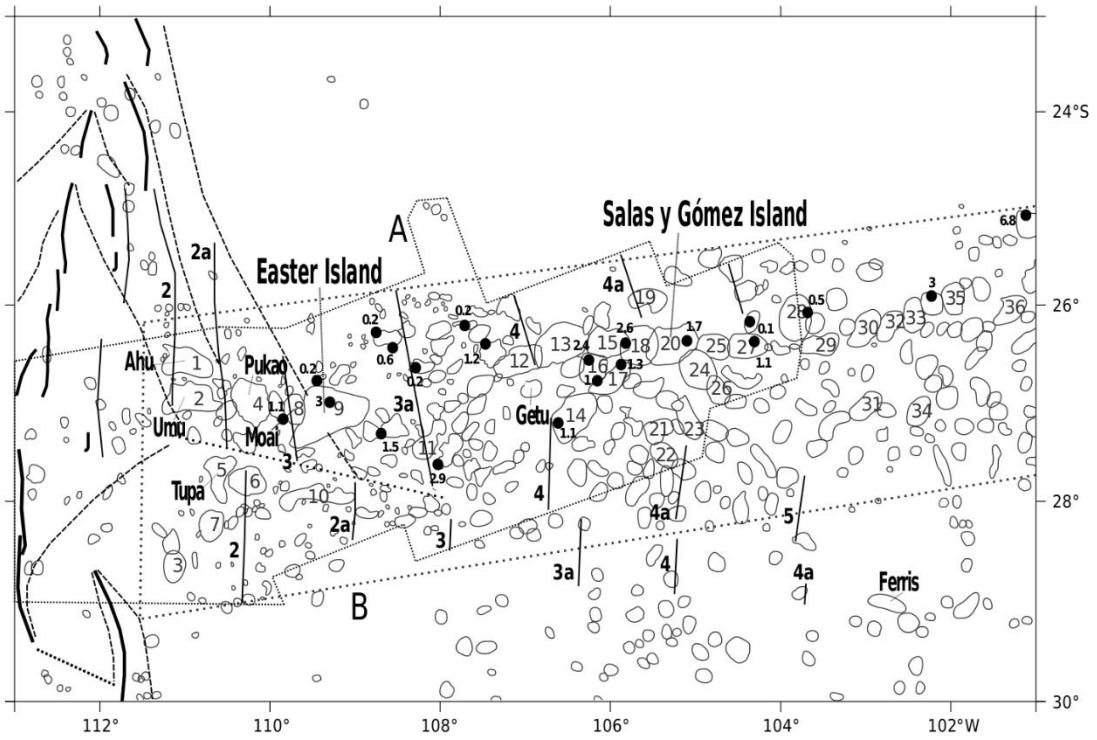

Figure 6. Basal areas of seamounts. The area "A" corresponds to that analyzed by Rappaport *et al.* (1997) and "B" for this work. Magnetic chrona (large bold numbers) are indicated. Rock sampling points (black circles) with their ages (small numbers) are also shown according the compilation of Naar *et al.* (2002).

On the other hand, in the sector around Easter Island, the seamounts tend to be elongated until 108.5°W, with the same strike of Easter Fracture Zone (Figs. 5-6). Between the two areas described, the shapes of the seamounts tend to elongate with a strike NE-SW, similar to small elevations that come out from the Rapa Nui alignment and show this same trend (such as the Easter Southeast elevation). By contrast the smaller seamounts outside area B of Figure 6 are more circular and isolated, not following a clear pattern in their spatial distribution.

In order to find a relationship between height, basal area and volume, 36 seamounts (and islands) were analyzed (Table 1), finding an average height of 2142 m, a minimum height of 1126 m and maximum height of 3434 m. The average value of the heights agrees with the value showed by Gálvez-Larach (2009) for the seamounts considered by him in the total extension of the chain. For basal area, the average was 1070 km^2, with a minimum of 500 km^2 and a maximum of 2180 km^2. The average volume was 817 km^3, the minimum was 258 km^3 and the maximum was 2370 km^3. In general, heights between 1000 and 1500 m, and also between 2500 and 3000 m dominate, with almost the same number in each case. Only four seamounts (taking into account the islands) have heights over 3000 m. At the same time, these ones have the largest basal areas and volumes (Figs. 7-8). Moreover, the lowest seamounts (<~2300 m) tend to have similar basal areas and volumes. These tend to be dome shaped. On the other hand, for seamounts with heights larger than about 2300 m, the taller their heights, the larger their basal area and volume, giving them a shape closer to a cone, but being elongated laterally.

Figure 6 also shows the magnetic isochrones obtained by Rappaport *et al.* (1997). Moreover, ages have been added that were obtained from samples from various cruises and other sources, compiled by Naar (2002). The samples were obtained from large and medium size seamounts. Neither correlation is observed between the ages and the sizes of the seamounts, nor with the location and arrangement. In general, these are younger ages than the surrounding crust generated by seafloor spreading. For instance, the 3a isochrone corresponds to an age of ~5.8 Myr, but the adjacent seamounts have an age between 2.9 and 0.2 Myr. Easter Island seems to be the oldest site, not having the age progression as the trend that Rapa Nui Chain has. In effect, the seamounts located to the SE of Easter Island are younger.

Table 1. Results of morphometric measurements of the considered seamounts.

Assigned number to the seamount	Coordinates of the seamount top	Top depth (m)	Base depth (m)	Heigh (m)	Basal area (km^2)	Volume (km^3)
1 (Ahu)	26°37.02'S, 111°09.12'W	1652	2850	1198	1101	439.7
2* (Umu)	26°37.81'S, 111°00.58'W	1250	2745	1495	1402	698.7
3	28°40.72'S, 111°10.56'W	1433	3100	1667	948	526.8
4 (Pukao)	26°54.25'S, 110°15.61'W	261	3100	2839	2001	1893.6
5* (Tupa)	27°44.06'S, 110°35.71'W	920	2760	1840	915	561.2
6*	27°49.92'S, 110°08.24'W	1480	2760	1280	796	339.6
7	28°14.89'S, 110°44.64'W	1641	3000	1359	570	258.2
8 (Moai)	27°05.99'S, 109°41.77'W	623	3015	2392	500	398.7
9 (Easter Island)	27°05.29'S, 109°22.57'W	-434	3000	3434	2071	2370.6
10	27°59.66'S, 109°10.12'W	1606	3000	1394	710	329.9
11*	27°27.42'S, 108°10.79'W	1665	3020	1355	720	325.2
12	26°35.28'S, 107°14.84'W	1680	3250	1570	2084	1090.6
13	26°19.89'S, 106°31.97'W	228	3450	3222	2180	2341.3
14	27°05.53'S, 106°24.01'W	553	3225	2672	1547	1377.9
15*	26°26.61'S, 105°53.54'W	455	2870	2415	1566	1260.6
16*	26°39.97'S, 106°14.13'W	215	2475	2260	627	472.3
17*	26°45.74'S, 105°55.06'W	1080	2910	1830	620	378.2
18	26°24.72'S, 105°33.86'W	518	3150	2632	1006	882.6
19	25°57.84'S, 105°39.59'W	2174	3300	1126	701	263.1
20 (Salas y Gómez I.)	26°27.57'S, 105°22.07'W	-42	3135	3177	1828	1935.9
21	27°14.88'S, 105°28.49'W	1932	3100	1168	775	301.7
22*	27°33.04'S, 105°23.13'W	1180	3050	1870	551	343.5
23*	27°14.66'S, 105°04.27'W	1105	3125	2020	960	646.4
24	26°38.90'S, 104°55.68'W	709	3250	2541	1038	879.2
25*	26°24.81'S, 104°51.45'W	605	2890	2285	747	569.0
26	26°50.64'S, 104°46.81'W	1726	3300	1574	641	336.3
27	26°24.97'S, 104°36.95'W	1396	3400	2004	810	541.1
28*	26°07.71'S, 103°49.18'W	330	2835	2505	1229	1026.2
29	26°23.39'S, 103°36.98'W	1819	3100	1281	996	425.3
30*	26°10.63'S, 102°57.78'W	260	3110	2850	970	921.5
31	27°00.24'S, 102°59.05'W	482	3300	2818	1160	1089.6
32	26°10.56'S, 102°41.76'W	1205	3100	1895	931	588.1
33	26°02.90'S, 102°25.13'W	191	3000	2809	853	798.7
34	27°05.98'S, 102°25.20'W	819	3350	2531	954	804.9
35	25°52.60'S, 101°57.36'W	622	3200	2578	841	722.7
36	26°03.42'S, 101°19.43'W	55	3300	3245	1172	1267.7

* From Seamount Biogeosciences Network

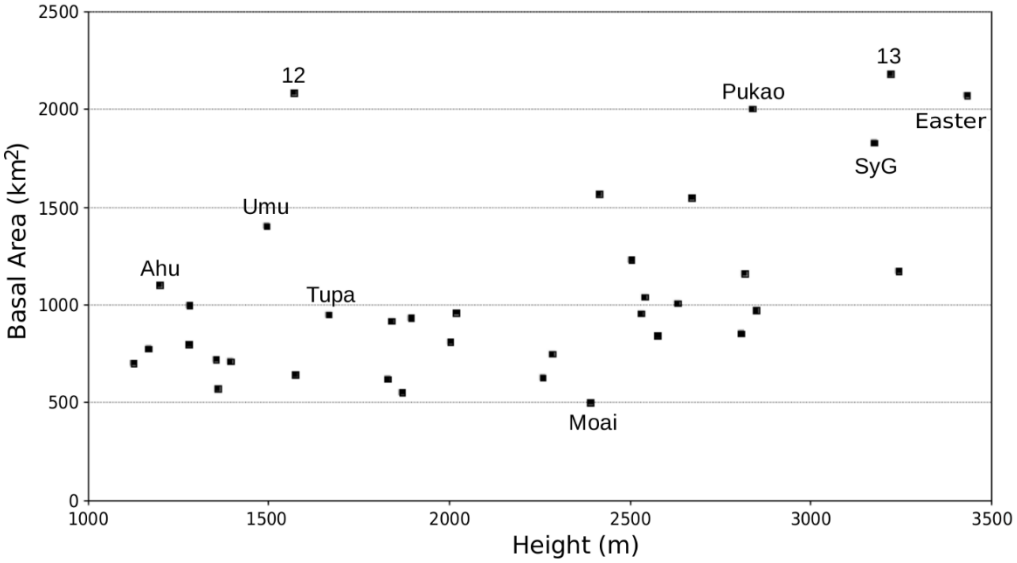

Figure 7. Basal area *vs.* maximum height of considered seamounts. Note that there is a clear trend of increasing basal area from the height of the Moai seamount. For altitudes below 2300 m there is no correlation between height and basal area.

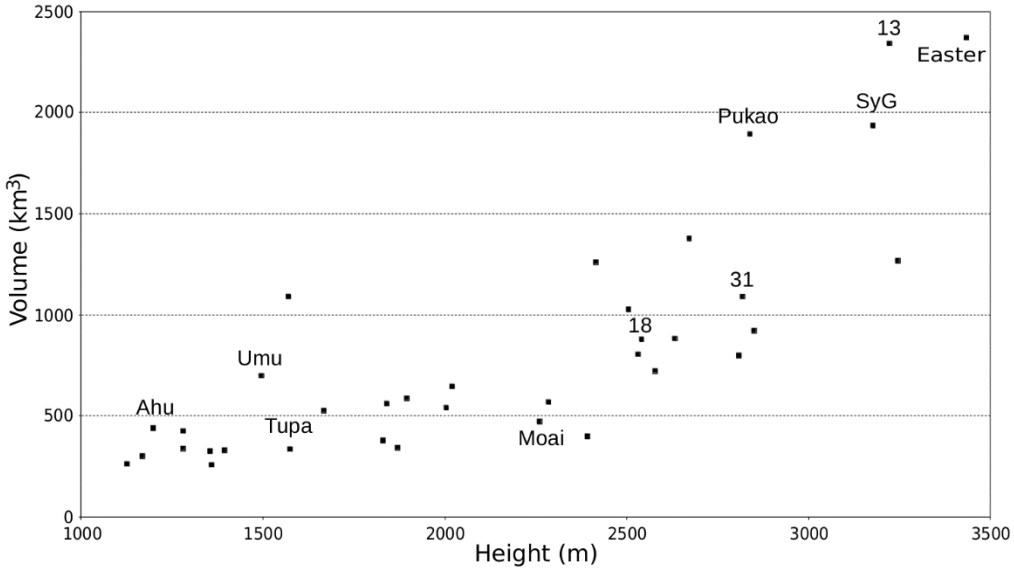

Figure 8. Volume *vs.* maximum height of considered seamounts. Note the increase in volume that from the Moai seamount height upward. For altitudes below 2300 m there is a low correlation between height and volume.

DISCUSSION

The morphologic pattern of the alignment and its relation with tectonics

The study region shows various types of morphological structures. Several of them tend to orientate or follow patterns of defined structures. These arrangements reflect the possible mechanisms that created them or their association with other tectonic phenomena. Because of the size of the Pacific Ocean Basin and because it represents the boundary between several plates, the most important morphologic feature is the East Pacific Rise. The Easter microplate is divided into a West Rift and an East Rift (Hey *et al*., 1985; Naar & Hey, 1986; Naar, 1992). The East Rift in the study area is separated in six segments suggesting that magmatic activity has not been continuous, both in space and time. The ridge segmentation, as well as the presence of a structural high just at its axis, are considered common characteristics for fast spreading ridges (Macdonald, 1989; Scheirer & Macdonald, 1995). Almost all the segments of the ridge in the study area

show a slight tendency to curve their tips towards the other ridge segment and to form OSCs. The two highest segments probably had more recent activity and with more magmatic volume, such that allowed for the taller height of these fractions. The trends oriented with the minor alignments identified are consistent with the propagating rift model (Hey *et al*., 1989).

The magmatic processes of the ridge affect and modify the topography. The features formed by the ridge are superimposed on top of those formed by other phenomena. In effect, to the north of Easter Island, the alignments tend to change their orientations to N-S. This behavior is expected for a situation of that changes from normal crust spreading to a situation dominated by the presence of pseudofaults, which in turn area created by the propagation of the ridge. In the southern sector of the Easter Fracture Zone (FZ), this dominant behavior is also reflected in the topographic features. The Easter FZ was recognized as a depression in the topography and also produces an offset in the magnetic anomalies. This fracture zone represents the trace of a transform fault of the mid-ocean ridge before the formation of the Easter Microplate more than 2 Myr ago (Hey *et al*., 1995; Martínez *et al*., 1997).

The large number of seamounts identified shows that volcanic activity is important inside the study region. We verify that seamounts align with characteristic trends according to their size and height, as opposed to what has been claimed by Rappaport *et al*. (1997), who argued that there was no clear pattern in their spatial distribution. In general, the largest seamounts tend to be aligned in an E-W direction, in some cases are forming continuous blocks, as in the Salas y Gómez Island sector. The trends of Easter Island together with Ahu and Umu can be associated to the Easter FZ. And this distinctive arrangement implies that the mechanisms that created or modified the distribution of this seamount chain were different to those of Salas y Gómez. In effect, the strike of the Salas y Gómez seamount chain is similar to that of other younger alignments in relation with the reorganization of the seafloor of the Nazca Plate 25 Myr ago (Tebbens & Cande, 1997; Tebbens *et al*., 1997). The other trends in the orientation of the alignments are difficult to associate to a particular tectonic process with the available data, but one could suspect that there are stresses exerted on the plate that can fracture or generate internal tension, which could be reflected in the elongation of the structures and the linear N-S or oblique arrangements.

Implications on the origin of the alignment

The simplest mechanism that explains the formation of the Easter Submarine Alignment is the hotspot. The chain of seamounts and islands extends from W to E near the ridge, in the Ahu and Umu volcanic fields, because from this point volcanic edifices are born and, additionally, in this area volcanoes should be active (Hagen *et al*., 1990). Therefore, the tendency is to locate the hotspot there. However, the necessary age progression towards the E is not fulfilled (at least within the study region), and contemporary volcanism exists at various points of the alignment (<3 Myr). The oldest adjacent seafloor, at the eastern side, is ~10-12 Myr old. Due to the complexity of tectonic processes, such as plate reorganizations, jumps in ridge activity, propagating rifts, generation of microplates, etc., it is evident that the assumption of a simple mechanism could not allow for the complex arrangement of topographic features, as well as the sizes involved and the morphologic characteristics.

The morphologic evidence has shown that two different areas exist: the sector of Easter Island and the one of Salas y Gómez Island, possibly related to different origins for both sites. Geochemical evidence (*e.g.*, Bonatti *et al*., 1977; Haase *et al.*, 1996; Kingsley *et al*., 2002; Simons *et al*., 2002) show mixtures of tholeiitic and alkaline basalts at various sites, so the hotpost should be beneath Salas y Gómez Island, in contrast to Haase *et al*. (1996) who claim that the hotspot should be close to Easter Island. Considering the hypothesis based on the geochemistry, one observes that the morphologic trends of the Salas y Gómez seamounts can be satisfactorily associated. It is possible that the hotspot is located more to the W of the island (at 107°W), given the shapes and strike of seamounts 12 and 13 (Fig. 6). The latter would be consistent with the proposition of Rappaport *et al*. (1997), who claim that the largest seamounts could only be formed by a hotspot mechanism. Moreover, the fact that Easter Island and other nearby seamounts have large volumes is also consistent with an additional magma supply coming from the ridge. In any case, the existence of a linear topographic connection among the islands allows the consideration that the hotspot would not be fixed in time, and rather would change its position. The latter would be consistent with the variability of the tectonic phenomena in the area.

No morphological evidence was found to support an origin by "leaking fracture zone" at least for the entire alignment. However, there could be volcanism in any site where the structure of the lithosphere would allow it. This could have happened in the Easter FZ, taking into account the strike of the structures.

CONCLUSIONS

In the study area depths between 2950 and 3700 m dominate, with an average depth of 3239 m. The Easter

Submarine Alignment is formed by seamounts and islands of various sizes arranged along a line, with a general strike of N85°E, similar to other alignments of the Nazca Plate with ages younger than 25 Myr. In the study area 514 seamounts were counted, showing that volcanic activity is important in this region, from which 334 had a basal area less than that of Moai, the reference seamount. In general, larger seamounts (>1000 m in height) tend to align themselves and have larger volumes whereas smaller seamounts tend to be distributed more randomly, with rounded or dome shapes. However, they have a general tendency to distribute themselves with an E-W arrangement with an elongation of their bases in this same direction.

The processes of the East Pacific Rise and others associated with the generation of Easter Microplate, such as overlapping spreading centers and propagating rifts reflect themselves in the topography adjacent to this mid-ocean ridge and are superimposed on top of other structures generated by different mechanisms. The results of the spatial distribution and sizes of the seamounts, shapes and arrangements of bases, differences in the topographic tendencies in the Easter Island and Salas y Gómez Island areas, together with geochemical and seafloor ages information, support the argument that the best mechanism to explains the origin of the volcanic chains is that of the existence of a hotspot caused by a mantle plume localized to the W of Salas y Gómez Island, probably at ~107°W. This plume could provide additional magmatic material towards the East Pacific Rise or the Easter Microplate through canalizations (Rodrigo, 2000), whose secondary branches could feed intermediate volcanoes between the East Pacific Rise and the hotspot. It is possible that there is another minor supply of material, through fractures in the crust due to the crustal weakening produce by the Easter Fracture Zone, for the Rapa Nui or Easter Chain in addition to the material coming from the previously described mechanisms.

ACKNOWLEDGEMENTS

The Pew Environment Group. The bathymetric data were downloaded from the website of the Geodetic Satellite Group of the Scripps Institution of Oceanography, University of California San Diego. Various maps shown in this paper were produced with GMT package obtained from SOEST, University of Hawaii, and with Mirone package from Joaquin Luis. To Chaynna Lodis, geology student at UNAB for her assistance in producing the figures and the statistics. Journal reviewers are kindly acknowledged by their constructive criticism.

REFERENCES

Amante, C. & B.W. Eakins. 2009. ETOPO1 1 Arc-Minute Global Relief Model: procedures, Data Sources and Analysis. NOAA Technical Memorandum NESDIS NGDC-24, 19 pp.

Baker, E.T., R.N. Hey, J.E. Lupton, J.A. Resing, R.A. Feely, J.J. Gharib, G.J. Massoth, F.J. Sansone, M. Kleinrock, F. Martínez, D.F. Naar, C. Rodrigo, D. Ohnenstiehl & D. Pardee. 2002. Hydrothermal venting along earth's fastest spreading center: East Pacific Rise, 27.5°-32.3°S. J. Geophys. Res., 17: EPM 2/1-14.

Bonatti, E., C.G. A. Harrison, D.E. Fisher, J. Honnorez, J.G. Schilling, J.J. Stipp & M. Zentilli. 1977. Easter Volcanic Chain (southeast Pacific): a mantle hot line. J. Geophys. Res., 82: 2457-2478.

Becker, J.J., D.T. Sandwell, W.H.F. Smith, J. Braud, B. Binder, J. Depner, D. Fabre, J. Factor, S. Ingalls, S.H. Kim, R. Ladner, K. Marks, S. Nelson, A. Pharaoh, R. Trimmer, J. Von Rosenberg, G. Wallace & P. Weatherall. 2009. Global bathymetry and elevation data at 30 arc seconds resolution: SRTM30 PLUS. Mar. Geod., 32: 355-371.

Clark, J.G. & J. Dymond. 1977. Geochronology and petrochemistry of Easter and Salas y Gómez islands: implications for the origin of the Salas y Gómez Ridge. J. Volcanol. Geotherm. Res., 2: 29-48.

Clouard, V. & A. Bonneville. 2001. How many Pacific hotspots are fed by deep-mantle plumes? Geology, 29: 695-698.

Gálvez-Larach, M. 2009. Montes submarinos de Nazca y Salas y Gómez: una revisión para el manejo y conservación. Lat. Am. J. Aquat. Res., 37(3): 479-500.

González-Ferrán, O. 1987. Evolución geológica de las islas chilenas en el océano Pacífico. In: J.C. Castilla (ed.). Islas oceánicas chilenas: conocimiento científico y necesidades de investigación. Universidad Católica de Chile, Santiago, 37-54 pp.

González-Ferrán, O.1994. Volcanes de Chile. Centro de Estudios Volcanológicos. Instituto Geográfico Militar, Santiago, 640 pp.

Haase, K.M. & C.W. Devey. 1996. Geochemistry of lavas from the Ahu and Tupa volcanic fields, Easter Hotspot, southeast Pacific: Implications for intraplate magma genesis near a spreading axis. Earth Planet. Sci. Lett., 137: 129-143.

Haase, K.M., C.W. Devey & S.L. Goldstein. 1996. Two-way exchange between the Easter mantle plume and the Easter Microplate spreading axis. Nature, 382: 344-346.

Hagen, R.A., N.A. Baker, D.F. Naar & R.N. Hey. 1990. A SeaMarc II survey submarine volcanism near Easter Island. Mar. Geophys. Res., 12: 297-315.

Hall, P.S. & C. Kincaid. 2004. Melting, dehydration, and the geochemistry of off-axis plume-ridge interaction, Geochem. Geophys. Geosyst., 5, Q12E18.

Hey, R.N. 1977. A new class of "pseudofaults" and their bearing on the plate tectonics: a propagating rift model. Earth Planet. Sci. Lett., 37: 321-325.

Hey, R.N., J.M. Sinton & F.K. Duennebier. 1989. Propagating rifts and spreading centers. In: E.L. Winterer, D.M. Hussong & R.W. Decker (eds.). The Eastern Pacific Ocean and Hawaii: Boulder, Colorado, Geological Society of America, The Geology of North America, N: 161-186.

Hey, R.N., D.F. Naar, M.C. Kleinrock, W.J. Phipps-Morgan, E. Morales & J.G. Schilling. 1985. Microplate tectonics along a superfast seafloor spreading system near Easter Island. Nature, 317: 320-325.

Hey, R.N., P.D. Johnson, F. Martínez, J. Korenaga, M.L. Somers, Q.J. Huggett, T.P. LeBas, R.I. Rusby & D.F. Naar. 1995. Plate boundary reorganization at a large-offset, rapidly propagating rift. Nature, 378: 167-170.

Hey, R.N., E. Baker, D. Bohnenstiehl, G. Massoth, M. Kleinrock, F. Martinez, D. Naar, D. Pardee, J. Lupton, R. Feely, J. Gharib, J. Resing, C. Rodrigo, F. Sansone & S. Walker. 2004. Tectonic and volcanic segmentation and controls on hydrothermal venting along Earth's Fastest active seafloor Spreading System, EPR 27°-32°S. Geochem. Geophys. Geosys., 5: Q12007.

Herron, E.M. 1972. Two small crustal plates in the South Pacific near Easter Island. Nature, 240: 35-37.

Kingsley, R.H. & J.G. Schilling. 1998. Plume-ridge interaction in the Easter-Salas y Gómez seamount chain-Easter microplate system: Pb isotope evidence, J. Geophys. Res., 103: 24159-24177.

Kingsley, R.H., J.G. Schilling, J.E. Dixon, P. Swart, R. Poreda & K. Simons. 2002. D/H ratios in basalt glasses from the Salas y Gómez mantle plume interacting with the East Pacific Rise: water from old D-rich recycled crust or primordial water from the lower mantle? Geochem. Geophys. Geosyst., 3(4): 1-26.

Lugo, J. 1986. Las estructuras mayores de la corteza terrestre. Universidad Autónoma de México, México, 133 pp.

Macdonald, K.C. 1989. Tectonic and magmatic processes on the East Pacific Rise. In: E.L. Winterer, D.M. Hussong & R.W. Decker (eds.). The Eastern Pacific Ocean and Hawaii. Geological Society of America, Boulder, Colorado, The Geology of North America, pp: 93-110.

Mammerickx, J. & D. Sandwell. 1986. Rifting of old oceanic lithosphere. J. Geophys. Res., 91: 1975-1988.

Martínez F., R.N. Hey & P.D. Johnson. 1997. The East ridge system 28.5°-32°S East Pacific Rise: implications for overlapping spreading center development. Earth Planet. Sci. Lett., 151: 13-31.

Menard, H.W. 1964. Marine geology of the Pacific. Mc Graw-Hill, New York, 271 pp.

Menard, H.W. & T. Atwater. 1968. Changes in direction of sea-floor spreading: Nature, 219: 463-467.

Morgan, W. 1972. Plate motions and deep mantle convection. Geol. Soc. Am. Mem., 132: 7-22.

Morales, E. 1984. Geografía de los fondos marinos. Geografía de Chile, Tomo VI. Instituto Geográfico Militar, Santiago, 206 pp.

Morales, E. & C. Rodrigo. 1993-1994. Antecedentes generales de la distribución y abundancia de montes submarinos en el Pacífico. Rev. Geogr. Valpo., 24-25: 103-120.

Naar, D.F. 1992. Microplates. Encyclopedia of Earth System Science. Academic Press, 3: 231-236.

Naar, D.F. 2002. Drift Expedition Leg 6 Web Site, http://www.soest.hawaii.edu/pwessel/drft06rr/. Reviewed: 5 April 2014

Naar, D.F. & R.N. Hey. 1986. Fast rift propagation along the East Pacific Rise near Easter Island. J. Geophys. Res., 91: 3425-3438.

Naar, D.F. & R.N. Hey. 1991. Tectonic evolution of the Easter Microplate. J. Geophys. Res., 96: 7961-7993.

Naar, D.F., R. Batiza, R. Poreda & J.G. Schilling. 1993. Final cruise report for the R/V Melville Gloria Expedition Legs 6 and 7. Gloria and geochemical investigations of the Easter Seamount Chain, 36 pp.

Okal, E. & A. Cazenave. 1985. A model for the plate tectonic evolution of the east-central Pacific based on SEASAT investigations. Earth Planet. Sci. Lett., 72: 99-116.

Pilger, R.H. & D.W. Handschumacher. 1981. The fixed-hotspot hipothesis and origin of The Easter-Salas and Gómez-Nazca trace. Geol. Soc. Am. Bull., 92: 437-446.

Rappaport, Y., D.F. Naar, C.C. Barton, Z.J. Liu & R.N. Hey. 1997. Morphology and distribution of seamounts surrounding Easter Island. J. Geophys. Res., 102: 24713-24728.

Ray, J.S., R.A. Duncan, J. Ray, P. Wessel & D.F. Naar. 2012. Chronology and geochemistry of Lavas from the Nazca Ridge and Easter Seamount Chain: an ~30 Myr Hotspot Record. J. Petrol., 53: 1417-1448.

Richter, F.M. 1973. Convection and the large-scale circulation of the mantle, J. Geophys. Res., 78(35): 8735-8745.

Rodrigo, C. 1994. Características morfológicas, geológicas y geofísicas del Alineamiento Submarino de Pascua. Tesis de Oceanografía. Pontificia Universidad Católica de Valparaíso, Valparaíso 150 pp.

Rodrigo, C. 2000. Estructura de la litosfera en el área de la isla de Pascua, mediante la interpretación de datos batimétricos y potenciales. Tesis de Maestría en Ciencias de la Tierra mención Geofísica Aplicada. Centro de Investigación Científica y de Educación Superior de Ensenada, Ensenada, 215 pp.

Rodrigo, C. & L. Lara. 2014. Plate tectonics and the origin of the Juan Fernández Ridge: analysis of bathymetry and magnetic patterns. Lat. Am. J. Aquat. Res., 42(4): 907-917.

Sandwell, D.T., E.L. Winterer & J. Mammerickx. 1995. Evidence for diffuse extension of the Pacific Plate from Pukapuka ridges and cross-grain gravity lineations. J. Geophys. Res., 100: 15087-15099.

Scheirer, D.S. & K.C. Macdonald. 1995. Near axis seamounts on the flanks of the East Pacific Rise, 8°N to 17°N. J. Geophys. Res., 100: 2239-2259.

Schilling, J.G., H. Sigurdsson, A.N. Davis & R.N. Hey. 1985. Easter microplate evolution. Nature, 317: 325-331.

Searle, R.C. 1989. Location and segmentation of the Cocos-Nazca spreading centre west of 95ºW. Mar. Geophys. Res., 11: 15-26.

Received: 10 May 2014; Accepted: 8 September 2014

Searle, R.C., R.T. Bird, R.I. Rusby & D.F. Naar. 1993. The development of two oceanic microplates: Easter and Juan Fernandez microplates, East Pacific Rise. J. Geol. Soc., 150: 965-976.

Simons, K., J. Dixon, J.G. Schilling, R. Kingsley & R. Poreda. 2002. Volatiles in basaltic glasses from the Easter-Salas y Gómez Seamount Chain and Easter Microplate: implications for geochemical cycling of volatile elements, Geochem. Geophys. Geosyst., 3(7): 1-29.

Smith, W.H.F. & P. Wessel. 1990. Gridding with continuous curvature splines in tension. Geophysics, 55: 293-305.

Smith, W.H.F. & D.T. Sandwell. 1997. Global seafloor topography from satellite altimetry and ship depth soundings. Science, 277: 1956-1962.

Tebbens, S.F. & S.C. Cande. 1997. Southeast Pacific tectonic evolution from early Oligocene to Present. J. Geophys. Res., 102: 12061-12084.

Tebbens, S.F., S.C. Cande, L. Kovacs, J.C. Parra. J.L. LaBrecque & H. Vergara. 1997. The Chile ridge: a tectonic framework. J. Geophys. Res., 102: 12035-12059.